Enhanced Autophagy in the Kidney of AQP11 Null Mice Developing Polycystic Kidneys

Yasuko Tanaka [1,*], Mayumi Watari [1], Tatsuya Saito [1], Yoshiyuki Morishita [2] and Kenichi Ishibashi [1]

[1]   Department of Pathophysiology, Faculty of Pharmacy, Meiji Pharmaceutical University, 2-522-1 Noshio, Kiyose, Tokyo 204-8588, Japan; mayuwata1204@icloud.com (M.W.); tsaito@my-pharm.ac.jp (T.S.); kishiba@my-pharm.ac.jp (K.I.)

[2]   Department of Nephrology, Jichi Medical University, Saitama Medical Center, Saitama 330-8503, Japan; ymori@jichi.ac.jp

*   Correspondence: ystanaka@my-pharm.ac.jp; Tel.: +81-42-495-8506; Fax: +81-42-495-8612

Abstract: Aquaporin-11 (AQP11) is an intracellular water channel expressed at the endoplasmic reticulum (ER) of the kidney proximal tubule. Its gene disruption in mice leads to intracellular vacuole formation at one week old and the subsequent development of polycystic kidneys at three week old. As the damaged proximal tubular cells with intracellular vacuoles later form cysts, autophagy may play a role in their survival. We examined the autophagy activity before and after the development of cysts in AQP11(−/−) kidneys. We first observed an enhanced expression of LC3 gene (Map1lc3b) as well as other autophagy-related genes in AQP11(−/−) mice by quantitative PCR analysis. We then examined the formation of autophagosomes visualized by a green fluorescent fusion protein, GFP-LC3 in its transgenic mice. The expression of GFP-LC3 puncta was increased in the proximal tubule of AQP11(−/−) mice before the cyst formation. Interestingly, they were also observed in the cyst-lining epithelial cell. Further PCR analyses revealed the enhanced expression of apoptosis- and ER stress-related caspase genes before and after the cyst formation suggesting that ER stress may have enhanced autophagy. We conclude that autophagy will play an important role in the development and the survival of the kidney cysts in AQP11(−/−) mice.

Keywords: proximal tubule; LC3; ER stress; apoptosis; PKD

1. Introduction

Aquaporin-11 (AQP11) is a water channel, which is expressed widely in the body [1,2]. Unlike other aquaporins, it is not expressed at the plasma membrane but at the membrane of intracellular organelles such as the endoplasmic reticulum (ER) [1,2]. As its plasma membrane expression is limited, the results of its functional studies have been controversial. Some studies have revealed water and glycerol transport functions [3,4,5], while the other has reported no water transport activity [2]. Interestingly, the gene disruption in mice have led to intracellular vacuole formation in the proximal tubule at one week after birth suggesting its vital role in the kidney development and function [1]. As AQP11 is selectively expressed in the ER of proximal tubular cells [1], AQP11 may play an important role in the ER and the ER dysfunction may have caused the cyst formation. Very recently, the role of AQP11 in the glycosylation and the trafficking of polycystin-1 (PC-1) from the ER to the plasma membrane has been reported [6]. PC-1 is a responsible gene product for autosomal dominant polycystic kidney disease (ADPKD) in human. The results suggest that the cyst formation in AQP11 null (AQP11(−/−)) mice may be caused by the defective trafficking of PC-1.

We previously reported the up-regulation of the genes involved in ER stress and apoptosis in the kidney of AQP11(−/−) mice [7]. Increased apoptosis has been observed in some animal models of polycystic kidneys as well [8–10], in which initial apoptosis is generally followed by increased cell proliferation and cyst formation. However, the causal relationship between apoptosis and cell proliferation is not clear. Interestingly, enhanced autophagy also has been observed in another

polycystic kidney disease model [11]. It is possible that autophagy may facilitate cell survival but not be enough to support its full recovery, and thereby leading to an aberrant cell proliferation with eventual cyst development.

Autophagy is a general term used for describing the degradation of cytoplasmic components within lysosomes [12], which will be important for cell survival by clearing damaged proteins and organelles from the cytoplasm and recycling their contents via a lysosomal pathway. In the kidney, autophagy has been shown to be an important mechanism for cellular homeostasis and survival during stressed pathologic conditions, such as ischemia-reperfusion injury and cisplatin-cytotoxicity [13–15]. Thus, the induction of autophagy will be necessary for the damaged vacuolated cells in the AQP11(−/−) kidney to survive and recover even though they are transformed to cyst epithelia of polycystic kidneys.

Three types of autophagy (macroautophagy, microautophagy, and chaperone-mediated autophagy) have been identified [12]. The most widely examined one is macroautophagy which is mediated by a unique double-membraned organelle, autophagosome [12]. As LC3 (Microtubule-associated protein light chain 3) has been specifically identified at the autophagosomal inner membrane, green fluorescent protein GFP-LC3 has been used as a marker for visualizing autophagy in vivo [16].

The purpose of the current study was to examine the autophagy activity in the AQP11(−/−) kidney to get an insight into the mechanism for the development of polycystic kidneys. To monitor autophagy in vivo, we introduced GFP-LC3 as a marker for autophagy in AQP11(−/−) mice by crossing them with GFP-LC3 transgenic mice. We found enhanced autophagy throughout the development of the proximal tubule from vacuolated cells to cyst epithelia.

2. Results

2.1. Autophagy-Related Genes in the AQP11(−/−) Kidney

We first compared the expression levels of autophagy-related genes in the kidney of AQP11(−/−) mice with that of the wild type by qRT-PCR. We examined the mRNA of micro tubule-associated protein 1 light chain 3b (Map1lc3b) which is an isoform of LC3 attached to autophagosomes. We found the up-regulation of Map1lc3b in AQP11(−/−) mice at the age of both 2 and 8 weeks after birth (Figure 1A).

We further investigated whether autophagy was enhanced in the kidney of AQP11(−/−) mice by western blotting (Figure 1B). LC3-II (active form) is known to increase more than LC3-I (inactive form) in enhanced autophagy. The band of LC3-I (18kDa) was much stronger than LC3-II (16kDa) in wild mice, whereas the band of LC3-II was stronger than LC3-I in AQP11(−/−) mice. The results clearly indicated that autophagy was enhanced in the kidney of AQP11(−/−) mice.

To confirm the enhanced autophagy activity in AQP11(−/−) mice, we further examined the expression of other autophagy-related genes, Beclin1 (Becn1), autophagy related 5 (Atg5) and sequestosome 1 (Sqstm1/p62) that are related to early autophagosome formation. The expression levels of Becn1 and Atg5 mRNA were up-regulated in the AQP11(−/−) kidney progressively from 2 to 8 week old, while Sqstm1 was 2-fold higher in the AQP11(−/−) kidney at the age of both 2 and 8 weeks old (Fig. 2A). The difference of the level of these autophagy related gene expression was up-regulated in the cortex of AQP11(-/-) mice relative to wild mice, even if it was isolated from each kidney to the cortex and the medulla (Supplemental Information). As a marker for late autophagosome formation, we compared the expression of lysosomal-associated membrane protein 1 (Lamp1) and lysosomal-associated membrane protein 2 (Lamp2). We found that all these genes were up-regulated in the AQP11(−/−) mice at the age of both 2 and 8 weeks (Figure 2B). Therefore, the increase of Map1lc3b will not be due to the blocking of lysosomal fusions but to the enhanced activity of autophagy. As the intracellular vacuoles are formed at the age of 1–2 weeks and the cysts develop subsequently at 3–4 weeks [1], the results indicated the enhanced autophagy activity before and after the cyst formation in the kidney of AQP11(−/−) mice.
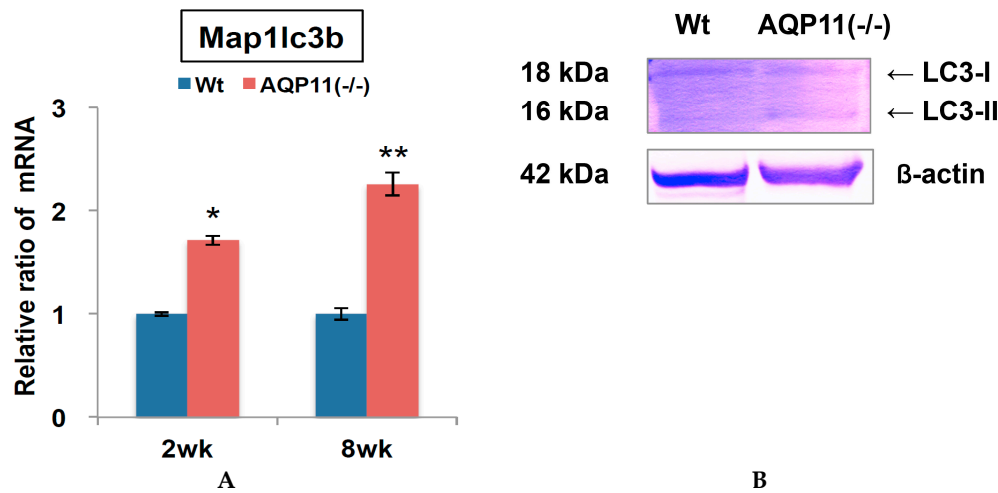
Figure 1. Quantitative reverse transcription polymerase chain reaction (qRT-PCR) analysis and western blotting analysis of an autophagy-related gene and protein in the kidney. (**A**) The expression levels of Map1lc3b, an autophagy-related gene, were compared between the kidneys of AQP11(−/−) mice and wild mice at 2 weeks (wk) and at 8 weeks. The expression level in the age-matched wild type kidney is arbitrarily normalized to1. The results are shown by the mean +/− SD. * $p < 0.005$ and ** $p < 0.025$ as compared with wild type. ($n = 5$ per group in 2 week old, $n = 3$ per group at 8 week old mice.); (**B**) The kidney expression of LC3 protein separated into LC3-I and LC3-II was compared between AQP11(−/−) mice and wild mice (Wt) at 3 weeks. The band of β-actin was used as an internal control. Similar observations were made in three separate sets of experiments.
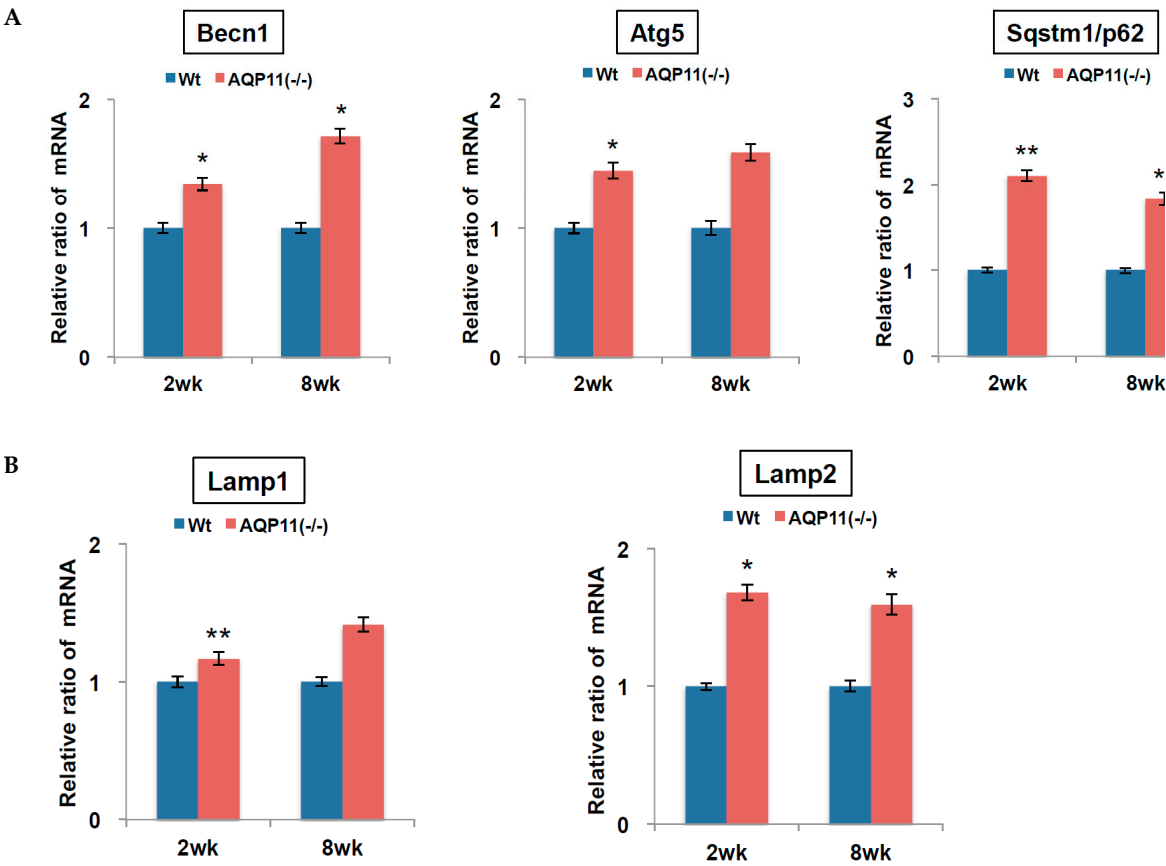
Figure 2. Quantitative analysis of autophagy-related genes in the kidney. All genes were compared by qRT-PCR between AQP11(−/−) mice and wild type mice (Wt) at 2 week (wk) old and at 8 week old. The expression level in the age-matched wild type kidney is arbitrarily normalized to 1. Individual

genes were examined as follows: (**A**) Becn1, Atg5, and Sqstm1/p62 as a marker for early autophagosome; (**B**) Lamp1 and Lamp2 a marker for late autophagosome. The results are shown by the mean +/− SD. * $p < 0.005$ and ** $p < 0.025$ as compared with wild type. (n = 4 to 5 pergroup at 2 week old, n = 3 per group at 8 week old mice.).

2.2. Autophagy Analysis in the AQP11(−/−) Kidney

To examine autophagy at a cellular level, we compared the amount of autophagosomes visualized by fluorescent puncta of GFP-LC3 in wild and AQP11(−/−) kidneys [16,17]. At the age of 2 weeks, just before the cyst formation, the number of GFP-LC3 puncta was increased in the cortex (Figure 3G). At a higher magnification, GFP-LC3 puncta were localized at proximal tubular cells, which were more intense in the AQP11(−/−) mice (Figure 3J) than in the wild type (Figure 3D). More GFP-LC3 puncta were observed at 7 week old when the cyst formation was completed (Figure 4G–L). Slight fluorescence in the wild type may be due to a nonspecific GFP expression as it was not in the form of puncta but in homogenous broader signals (Figure 4A–F). A distal tubule (indicated by asterisks in Figure 4I) displayed minimum autophagy activities. Therefore, AQP11(−/−) mice had an enhanced autophagy activity before and after the cyst formation in agreement with the results by qRT-PCR (Figure 1A).
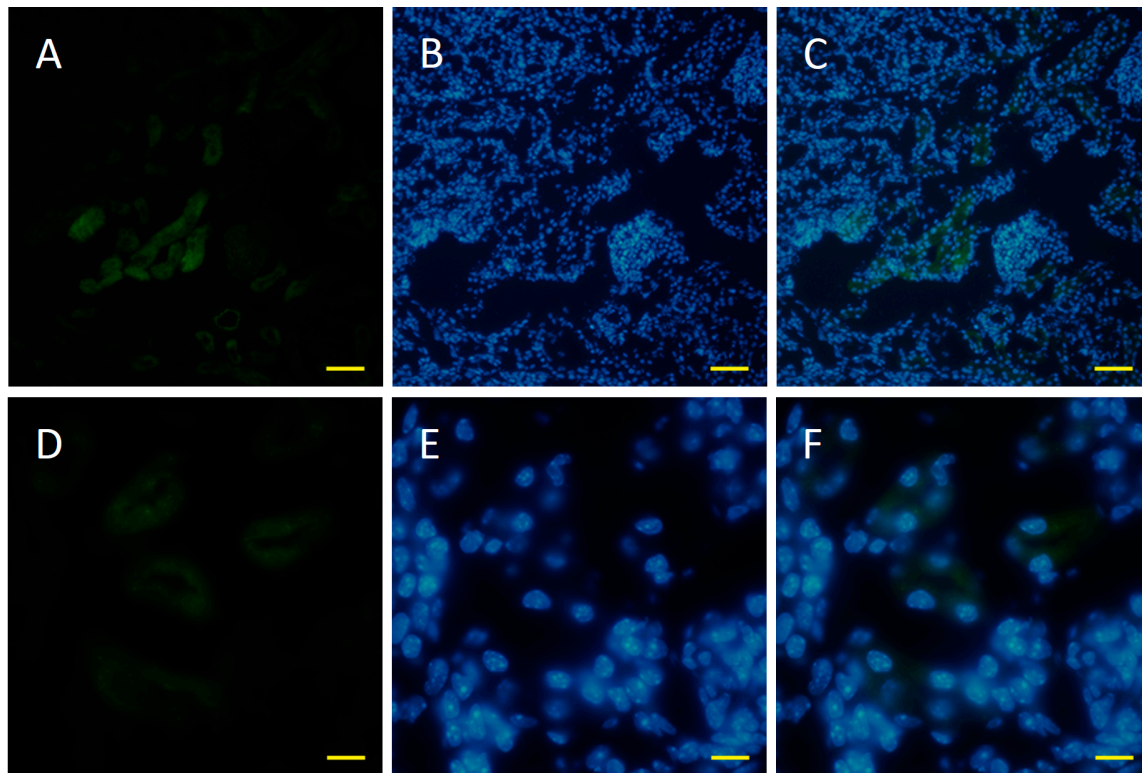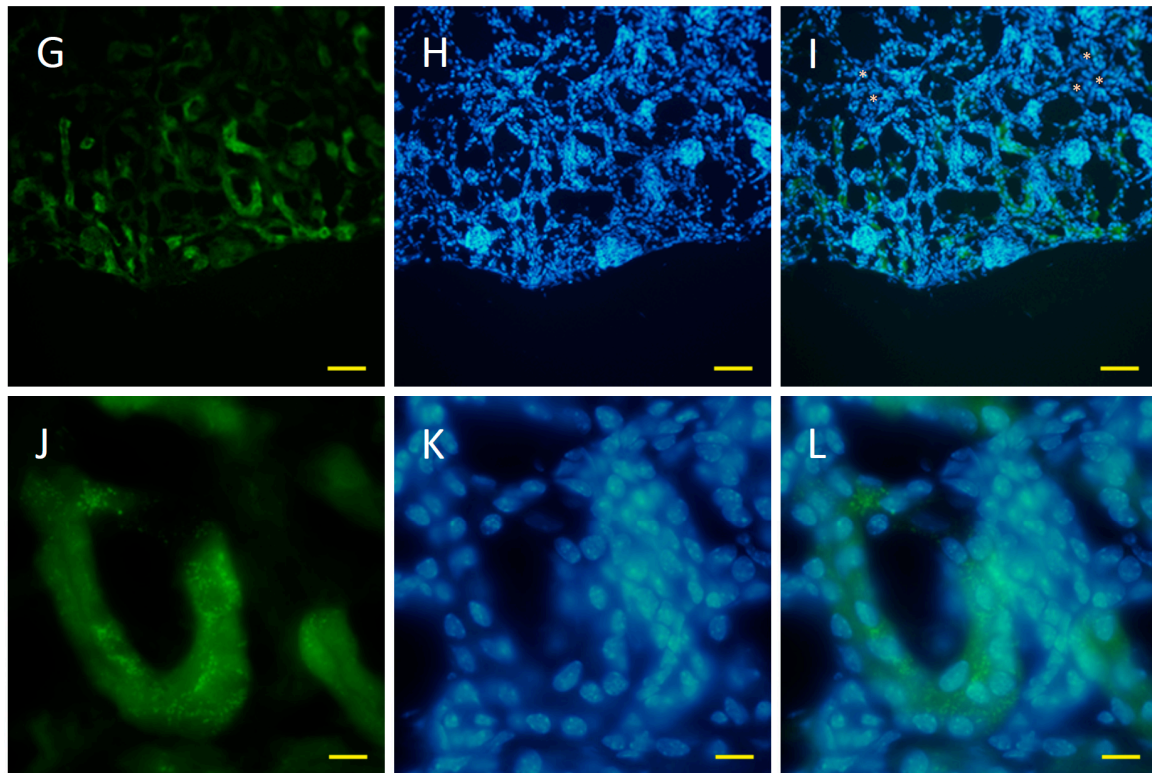
Figure 3. Fluorescent microscopy of the kidney cortex of GFP-LC3 transgenic mice that were crossed with AQP11 knockout orwild-type mice at 2 week old. Green fluorescence shows GFP-LC3 (**A,D,G,J**), while blue fluorescence indicates nucleic staining with DAPI (**B,E,H,K**). Both images are merged (**C,F,I,L**); **A–F** are from wild-type mice and **G–L** are from AQP11 knockout mice; **A–C** and **G–H** are at the higher magnification, while **D–F** and **J–L** are at the higher magnification, with bars indicating 50 and 10 μm length, respectively. The asterisks indicate the distal tubule (**I**). Similar observations were made in three separate sets of experiments.
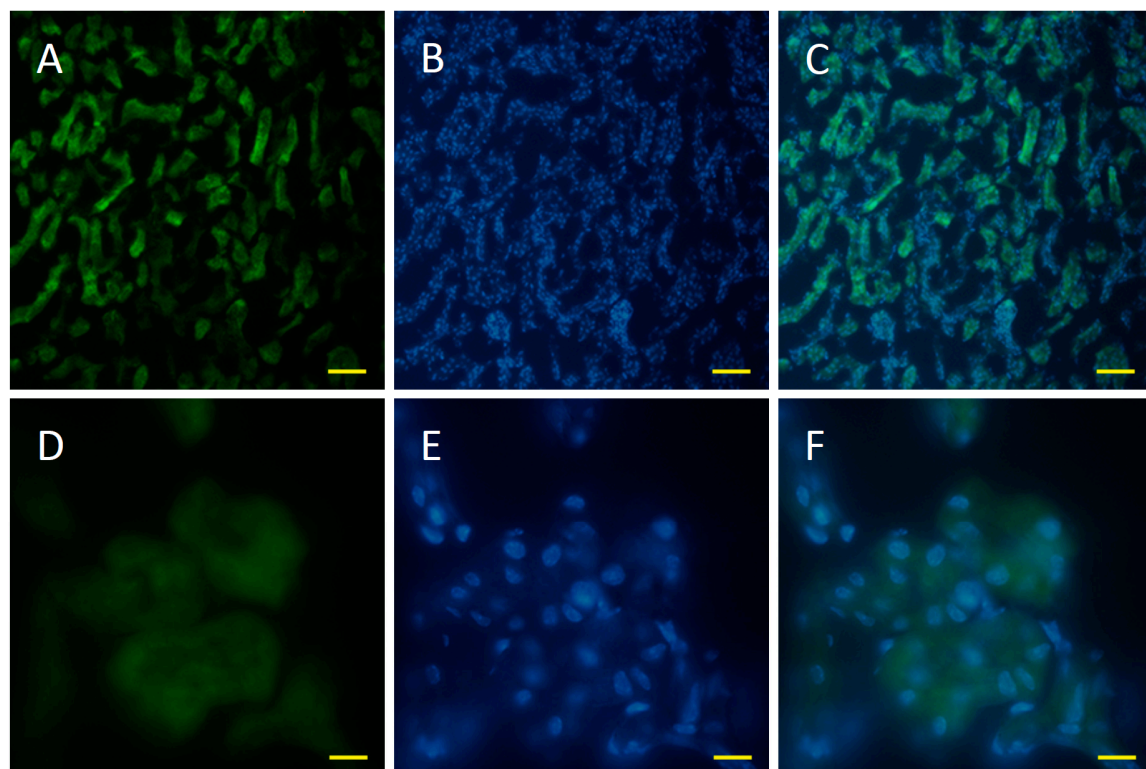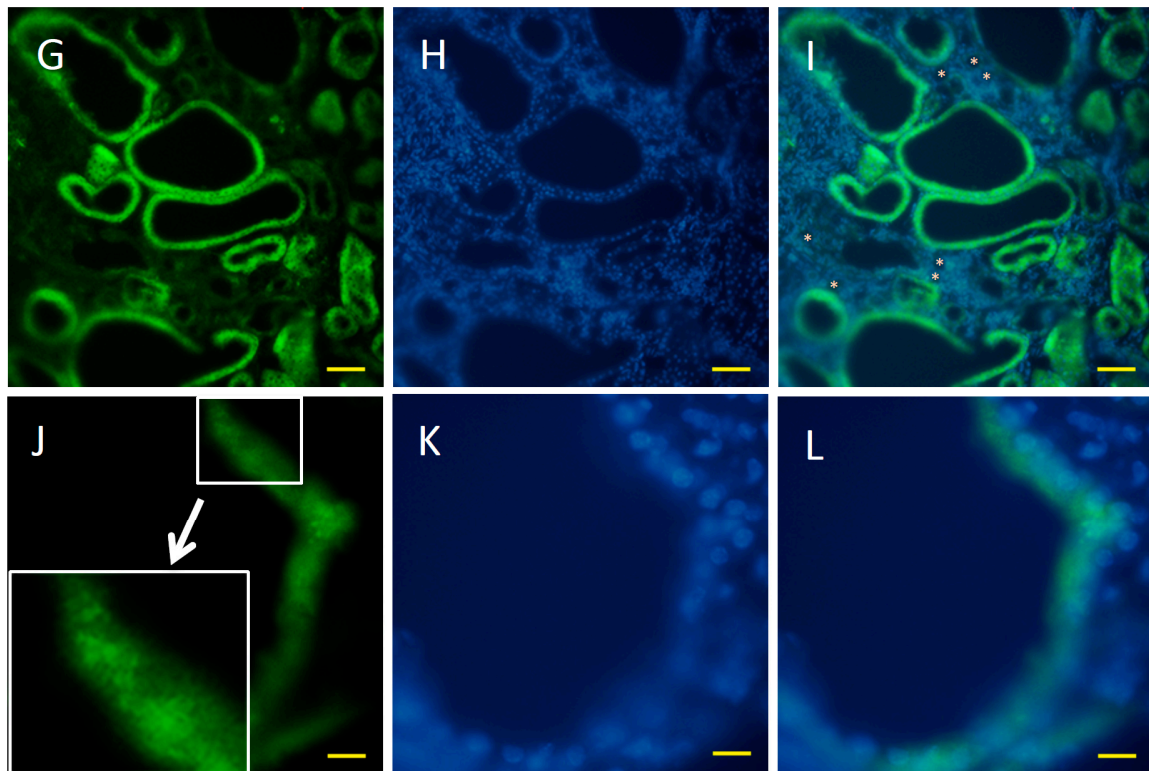
Figure 4. Fluorescent microscopy of the kidney cortex of GFP-LC3 transgenic mice that were crossed with AQP11 knockout or wild-type mice at 7 week old. Green fluorescence shows GFP-LC3 (**A,D,G,J**), while blue fluorescence indicates nucleic staining (**B,E,H,K**). Both images are merged (**C,F,I,L**); **A–F** are wild-type and **G–L** are AQP11 knockout mouse; **A–C** and **G–H** are at the lower magnification, while **D–F** and **J–L** are at the higher magnification. The asterisks indicate the distal tubule (**I**). The left lower frame of J showed enlarged puncta of GFP which were expressed in proximal tubule. Bars indicate 50 and 10 μm length at each magnification. The asterisk indicated the distal tubule. Similar observations were made in three separate sets of experiments.

2.3. The Expression of Apoptosis- and ER Stress-Related Genes

To get insights into the cause of the enhanced autophagy activity in the AQP11(−/−) kidney, we further examined the expression of genes related to apoptosis, inflammation and ER stress which will induce autophagy. We compared the mRNA levels of caspase family in the kidney by qRT-PCR as they will be markers for these events in the cell: caspase 3 (Casp3) and caspase 8 (Casp8) are indicators for the effector and the initiator of apoptosis, respectively; caspase 1 (Casp1) and caspase 4 (Casp4) are indicators for active inflammation; caspase12 (Casp12) is an indicator for ER stress. The mRNA expression levels of Casp3 and Casp8 were enhanced significantly at the age of 2 weeks and further at 8 weeks ~~old~~ in the AQP11(−/−) kidney (Figure 5A), suggesting an augmented apoptotic activity. The mRNA expression level of Casp1 was increased by 5 folds at the age of 2 weeks and by 12 folds at 8 weeks. Much higher expression levels were observed with Casp4 mRNA, by 7 folds at the age of 2 weeks and even more by 32 folds at 8 weeks. The both results suggest the presence of an active inflammation in AQP11(−/−) kidney. Finally, the mRNA expression levels of Casp12 was also enhanced by 9 folds at the age of 2 weeks and by 26 folds at 8 weeks, suggesting the presence of ER stress. Thus, all caspase genes examined were enhanced in the AQP11(−/−) kidney before and after the cyst formation with remarkably higher expressions of Casp1, Casp4 and Casp12. Taken together, our data suggested that the induction of autophagy in the AQP11(−/−) kidney was associated with apoptosis, inflammation, and ER stress.

Furthermore, we examined the genes related to the apoptosis induced by ER stress. Both activating transcription factor 4 (Atf4) and eukaryotic translation initiation factor 2 alpha (Eifak3) work in PERK-Atf4 pathway and thereby lead to apoptosis through the integrated ER stress response.

DNA-damage inducible transcript 3 (Ddit3/CHOP) is another downstream target of PERK-Atf4 pathway. We also examined the expression of heat shock protein 5 (Hspa5/Bip) which is activated by accumulated altered proteins in the ER. The mRNA expression levels of Atf4 and Eifak3 were 2-fold higher at the age of 2 weeks and 3-fold higher at 8 weeks (Figure 5B). Ddit3 was 6-fold higher at the age of 2 weeks and 3-fold higher at 8 weeks (Figure 5B). Hspa5 was 2.6-fold higher at the day of 2 weeks and 2-fold higher at 8 weeks (Figure 5B). The results further confirmed the enhanced ER stress activity before and after the cyst formation as suggested by the caspase expression (Figure 5A).
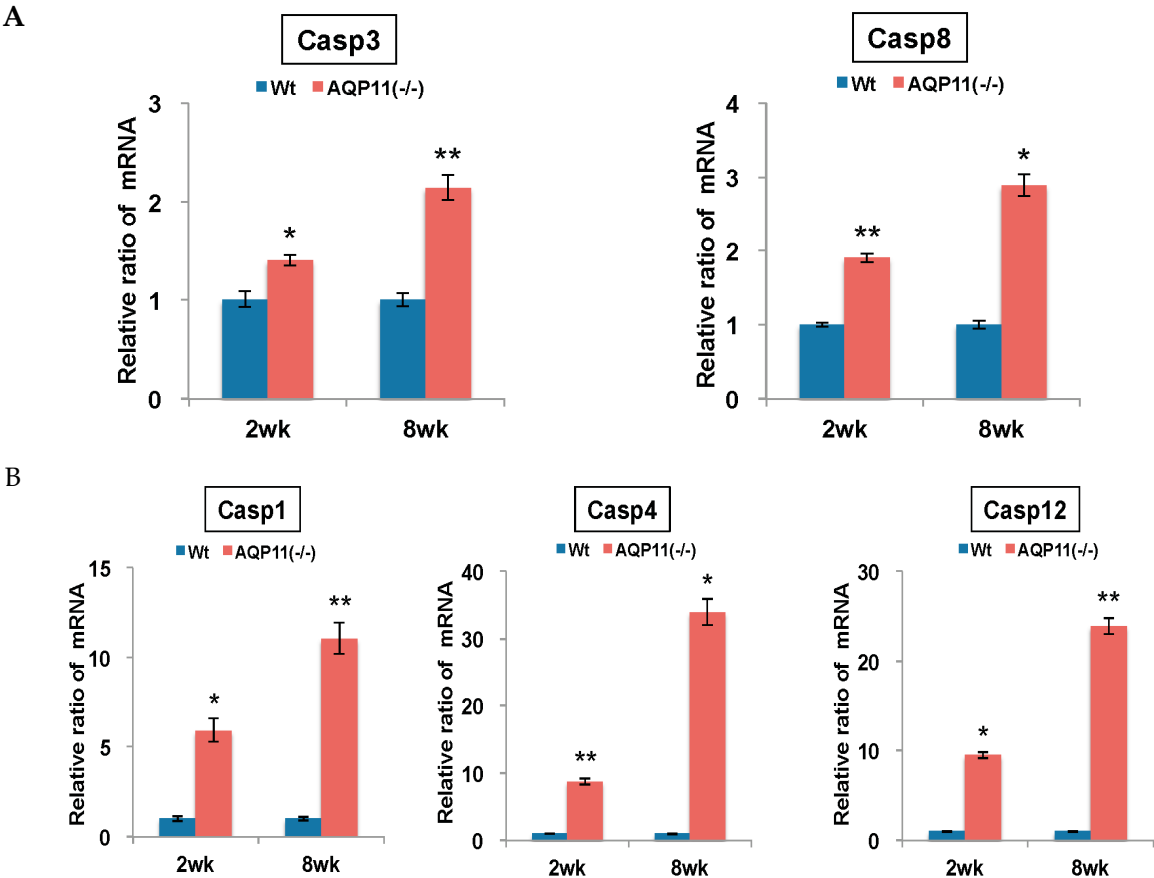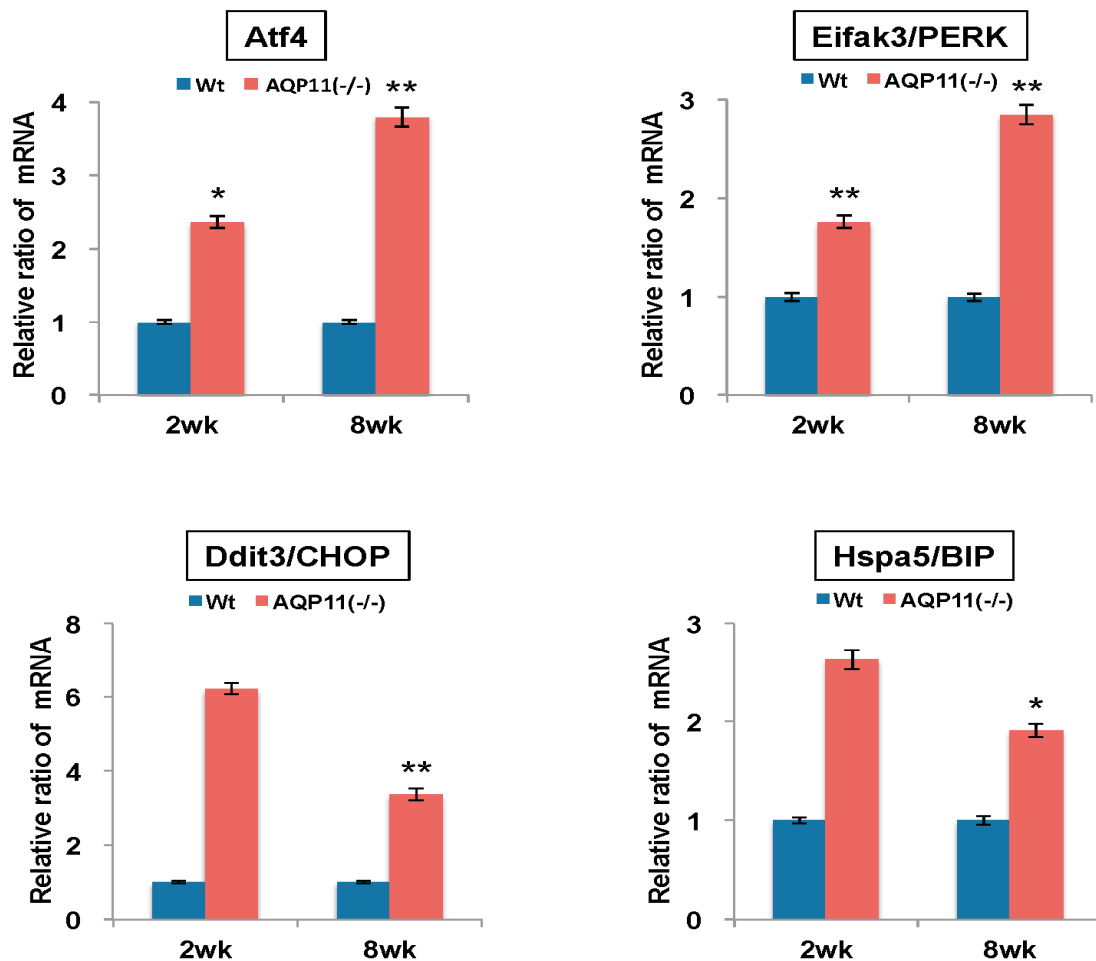
Figure 5. Quantitative analysis of mRNA expression in the kidney of AQP11(−/−) and wild type mice at 2 and 8 week old. All genes were compared by qRT-PCR between AQP11(−/−) mice and wild type mice (Wt) at 2 week (wk) old and at 8 week old. The expression levels in the age-matched wild type kidney are arbitrarily normalized to one. (**A**) Expression of inflammation, apoptosis, and ER-stress related Caspase family genes; (**B**) Expression of ER stress response genes related to Atf4/PERK signaling pathway. The results are shown by the mean +/− SD. The number of experiments was 4 to 3 at each week. * $p < 0.005$ and ** $p < 0.025$ as compared with wild type. ($n = 4$ to 5 per group at 2 week old, $n = 3$ per group at 8 week old mice.)

3. Discussion

Here we reported for the first time that autophagy was enhanced in the kidney of AQP11(−/−) mice before and even after the cyst formation. The autophagy was most likely induced by ER stress with miss-processed proteins as suggested by the report that AQP11 expressed at the ER is important for PC-1 trafficking to the plasma membrane with abnormal glycosylation [6]. As the proximal tubule suffers from extensive cell damage with intracellular vacuoles in the absence of AQP11 before the cyst formation, higher autophagy activities will be necessary for the survival of these cells as previously reported in other kidney injury models [13–15]. Apoptosis may also be induced by ER stress to eliminate irreversibly damaged and dead cells from the tubule to support the recovery of the proximal tubule [7]. The relationship between autophagy and apoptosis is intriguing and worthy of further studies.

It was unexpected to find a lasting enhanced autophagy activity even after the cyst formation where active cell damages seem to be absent. In fact, our quantitative gene expression studies of several caspases revealed much higher expression of apoptosis and ER stress-related genes after the cyst formation. The results suggest that autophagy will be important for the survival of cyst epithelia as well as for vacuolated cells. It is possible that the cyst epithelium may also suffer from a cellular

damage in the absence of AQP11 further with diminished glomerular filtration and narrowed vessels by compressing cysts which eventually compromise the blood supply to the cyst epithelium. The progressive nature of renal failure in AQP11(−/−) mice suggests that the cyst epithelium may also need AQP11 to survive although the induced autophagy may not be enough to recover. In fact, an enhanced autophagy activity has also been reported in other polycystic kidney disease (PKD) models [11,13]. However, it is difficult to distinguish the initiation phase from the survival phase of the cyst epithelium as the effect of autophagy since both occur simultaneously and at different segments of the nephron in most PKD models. Selective and acute damages to the proximal tubule in our model will make the analysis much easier [1]. Alternatively, autophagy could have been induced by physical damages on blood vessels produced by expanded or cystic epithelia, which also induced ER stress and apoptosis. Further studies on the cause-effect relationship of autophagy and ER stress will be necessary to be clarified.

The cyst formation in our model will be initiated by a defective ER function since abnormal glycosylation of polycystin-1 (PC-1) have caused its defective transfer to the plasma membrane [6]. We assumed that ER stress induced by the absence of AQP11 may trigger apoptosis in the proximal tubule while some cells may survive by simultaneously induced autophagy to form cysts with a defective PC-1 function. Interestingly, the cyst epithelium still seems to need autophagy for its survival. More studies on the role of autophagy in the trafficking of PC-1 will be necessary to substantiate the above hypothesis. Further study will also be necessary to clarify the relationships between autophagy, apoptosis and ER stress as well as the cause-effect relationship as discussed above. If autophagy should be important for the survival of cysts, modulations of autophagy will be a novel therapy for suppressing the progression of PKD.

We conclude that autophagy was induced in the proximal tubule of AQP11(−/−) mice associated with enhanced apoptosis and ER stress, and autophagy will be important for the cyst formation and its survival.

4. Materials and Methods

4.1. Mice

AQP11(−/−) mice were generated in our laboratory as previously reported [1]. GFP-LC3 heterozygous transgenic mice were obtained from RIKEN Bio-Resource Center in Japan [16]. Heterozygous AQP11 knockout mice (AQP11(+/−)) were interbred with heterozygous GFP-LC3 transgenic mice to generate GFP-LC3 transgenic mice in the background of AQP11(−/−). The genotyping for both AQP11 and GFP-LC3 were determined by PCR as previously reported [1,16].

4.2. Quantitative Real-Time PCR

Mice were anesthetized with pentobarbital and the whole body was perfused via the left ventricle of the heart with diethyl pyrocarbonate treated PBS (DEPC-PBS). Kidneys were then harvested and immersed in RNA *later* (QIAGEN) until use. Total RNA was isolated using RNeasy Mini Kit (QIAGEN) and the aliquots of 50 ng were reverse transcribed with random primers according to the manufacturers' instructions. Then, quantitative RT-PCR (qRT-PCR) was performed on the cDNA in triplets by Light Cycler Nano (Roche) with Fast Start Essential DNA Green Master (Roche) following the manufacturer's instructions. The primer sets used in this study were summarized in Table 1. The relative amount of mRNA was calculated using GAPDH mRNA as an internal control with 2nd Derivative Maximum method. A relative ratio was calculated by the gene expression of AQP11(−/−) mice relative to wild type mice.

Table 1. Sequences of primers for qRT-PCR.

Genes	Forward	Reverse
Atf4	5'-aitgatggcttggccagtg-3'	5'-ccattttctccaacatccaatc-3'

Atg5	5'-aagtctgtccttccgcagtc-3'	5'-tgaagaaagttatctgggtagctca-3'
Becn1	5'-aggatggtgtctctcgaagatt-3'	5'-gatcagagtgaagctattagcactttc-3'
Casp1	5'-cccactgctgatagggtgac-3'	5'-gcataggtacataagaatgaactgga-3'
Casp3	5'-gaggctgacttcctgtatgctt-3'	5'-aaccacgacccgtccttt-3'
Casp4	5'-tgtcatctctttgatatattcctgaag-3'	5'-caaggttgcccgatcaat-3'
Casp8	5'-ttgaacaatgagatccccaaa-3'	5'-ccatttctacaaaaatttcaagcag-3'
Casp12	5'-gggaattagcacaggcaact-3'	5'-ttcttttcttctcagctacagcaa-3'
Ddit3/CHOP	5'-gcgacagagccagaataaca-3'	5'-gatgcacttccttctggaaca-3'
Eifak3/PERK	5'-ccttggtttcatctagcctca-3'	5'-atccagggaggggatgat-3'
GAPDH	5'-tgtccgtcgtggatctgac-3'	5'-cctgcttcaccaccttcttg-3'
Hspa5/BIP	5'-ctgaggcgtatttgggaaag-3'	5'-tcatgacattcagtccagcaa-3'
Lamp1	5'-cctacgagactgcgaatggt-3'	5'-ccacaagaactgccatttttc-3'
Lamp2	5'-aaggtgcaacctttaatgtgac-3'	5'-tgtcatcatccagcgaacac-3'
Map11c3b	5'-ccccaccaagatcccagt-3'	5'-cgctcatgttcacgtggt-3'
Sqstm1/p62	5'-agacccctcacaggaaggac-3'	5'-catctgggagagggactcaa-3'

4.3. Western Blotting

After perfused with phosphate buffered saline (PBS), kidneys were isolated from the mice and then homogenized with a galas-Teflon homogenizer in Radio-Immunoprecipitation Assay (RIPA) buffer (Wako). After centrifugation at $10,000\times g$ for 20 min at 4 °C, the supernatant was collected. The solubilized protein was added 4 × SDS buffer (12% SDS, 25% Glycerol, 150 mM Tris-HCl (pH 7.0), 0.05% Bromophenol Blue and 6% β-mercaptoethanol) and equilibrated at room temperature for 30 min. The proteins (10 μg) were subjected to SDS-PAGE (15% gel, ATTO) and transferred to a Hybrond-P polyvinylidene difluoride membrane (Amersham, Japan) by a semi-dry blotting apparatus. The membrane was blocked with 1% bovine serum albumin in TBST for 1hr at room temperature. The primary antibodies were rabbit anti-LC3 (MBL, PM036, 1:1000 dilution) and rabbit anti-β-actin (Abcam, ab25894, 1:10,000 dilution). The bands were visualized by ProtoBlot II AP System with Stabilized Substrate Kit (Promega, Japan, W3960).

4.4. Fluorescent Microscopy

Mice were perfused as above with 4% paraformaldehyde (PFA, Sigma-Aldrich, city, country) in PBS. Kidneys were then harvested and fixed in 4% PFA overnight. The fixed tissues were immersed in PBS containing 10%, 15% and 20% (w/v) sucrose in succession. Finally, the samples were embedded in OTC compound (Tissue-Tek, Sakura Finetek, Japan) and frozen at −30 °C until use. Cryosections were prepared in 8 μm thickness with the Leica CM1510S cryostat (LEICA). Nuclei were stained with 4', 6-diamidio-2-phenylindole (DAPI, Wako, Japan). GFP and DAPI fluorescent signals were detected by an inverted fluorescent microscope (OLYMPUS, IX71) with respective filters.

4.5. Statistical Analysis

Comparisons between the two groups were performed using unpaired Student's t-test. $*\ p < 0.005$ and $**\ p < 0.025$ were considered to indicate a statistically significant difference. All data are expressed as means +/− SD.

Acknowledgments: We thank S. Nakada for the technical assistance and S. Sasaki for the critical reading of the manuscript. This work was supported by JSPS KAKENHI Grant Numbers 24591243 and 15K09302 to K. Ishibashi.

Author Contributions: K.I., Y.T. and Y.M. conceived and designed the experiments; Y.T. and M.W. performed the experiments; Y.T. and T.S. analyzed the data; Y.T. and K.I. wrote the manuscript.

Conflict of interest: The authors declare no conflict of interest.

References

1. Morishita, Y.; Matsuzaki, T.; Hara-chikuma, M.; Andoo, A.; Shimono, M.; Matsuki, A. ; Kobayashi, K.; Ikeda, M.; Yamamoto, T.; Verkman, A.; et al. Disruption of aquaporin-11 produces polycystic kidneys following vacuolization of the proximal tubule. *Mol. Cell. Biol.* **2005**, *25*, 7770–7779.

2. Gorelick, D.A.; Praetorius, J.; Tsunenari, T.; Nielsen, S.; Agre, P. Aquaporin-11: A channel protein lacking apparent transport function expressed in brain. *BMC Biochem.* **2006**, *7*, 14, doi:10.1186/1471-2091-7-14.

3. Yakata, K.; Hiroaki, Y.; Ishibashi, K.; Sohara, E.; Sasaki, S.; Mitsuoka, K.; Fujiyoshi, Y. Aquaporin-11 containing a divergent NPA motif has normal water channel activity. *Biochim. Biophys. Acta* **2007**, *1768*, 688–693.

4. Yakata, K.; Tani, K.; Fujiyoshi, Y. Water permeability and characterization of aquaporin. *J. Struct. Biol.* **2011**, *174*, 315–320.

5. Madeira, A.; Fernández-Veledo, S.; Camps, M.; Zorzano, A.; Moura, T.F.; Ceperuelo Mallafré, V.; Vendrell, J.; Soveral, G. Human aquaporin-11 is a water and glycerol channel and localizes in the vicinity of lipid droplets in human adipocytes. *Obesity* **2014**, *22*, 2010–2017.

6. Inoue, Y.; Sohara, E.; Kobayashi, K.; Chiga, M.; Rai, T.; Ishibashi, K.; Horie, S.; Su, X.; Zhou, J.; Sasaki, S.; et al. Aberrant glycosylation and localization of polycystin-1 cause polycystic kidney in an AQP11 knockout model. *J. Am. Soc. Nephrol.* **2014**, *25*, 2789–2799.

7. Okada, S.; Misaka, T.; Tanaka, Y.; Matsumoto, I.; Ishibashi, K.; Sasaki, S.; Abe, K. Aquaporin-11 knockout mice and polycystic kidney disease animals share a common mechanism of cyst formation. *FASEB J.* **2008**, *22*, 3672–3684.

8. Moser, M.; Pscherer, A.; Roth, C.; Becker, J.; Mücher, G.; Zerres, K.; Dixkens, C.; Weis, J.; Guay-Woodford, L.; Buettner, R.; et al. Enhanced apoptotic cell death of renal epithelial cells in mice lacking transcription factor AP-2beta. *Genes Dev.* **1997**, *11*, 1938–1948.

9. Trudel, M.; D'Agati, V.; Costantini, F. C-myc as an inducer of polycystic kidney disease in transgenic mice. *Kidney Int.* **1991**, *39*, 665–671.

10. Veis, D.J.; Sorenson, C.M.; Shutter, J.R.; Korsmeyer, S.J. Bcl-2-deficient mice demonstrate fulminant lymphoid apoptosis, polycystic kidneys, and hypopigmented hair. *Cell* **1993**, *75*, 229–240.

11. Belibi, F.; Zafar, I.; Ravichandran, K.; Segvic, A.B.; Jani, A.; Ljubanovic, D.G.; Edelstein, C.L. Hypoxia-inducible factor-1α (HIF-1α) and autophagy in polycystic kidney disease (PKD). *Am. J. Physiol. Ren. Physiol.* **2011**, *300*, F1235–F1243.

12. Maiuri, M.C.; Zalckvar, E.; Kimchi, A.; Kroemer, G. Self-eating and self-killing: Crosstalk between autophagy and apoptosis. *Nat. Rev. Mol. Cell Biol.* **2007**, *8*, 741–752.

13. Huber, T.B.; Edelstein, C.L.; Hartleben, B.; Inoki, K.; Jiang, M.; Koya, D.; Kume, S.; Lieberthal, W.; Pallet, N.; Quiroga, A.; et al. Emerging role of autophagy in kidney function, diseases and aging. *Autophagy* **2012**, *8*, 1009–1031.

14. Periyasamy-Thandavan, S.; Jiang, M.; Wei, Q.; Smith, R.; Yin, X.M.; Dong, Z. Autophagy is cytoprotective during cisplatin injury of renal proximal tubular cells. *Kidney Int.* **2008**, *74*, 631–640.

15. Jiang, M.; Wei, Q.; Dong, G.; Komatsu, M.; Su, Y.; Dong, Z. Autophagy in proximal tubules protects against acute kidney injury. *Kidney Int.* **2012**, *82*, 1271–1283.

16. Mizushima, N.; Yamamoto, A.; Matsui, M.; Yoshimori, T.; Ohsumi, Y. In vivo analysis of autophagy in response to nutrient starvation using transgenic mice expressing a fluorescent autophagosome marker. *Mol. Biol. Cell* **2004**, *15*, 1101–1111.

17. Kuma, A.; Hatano, M.; Matsui, M.; Yamamoto, A.; Nakaya, H.; Yoshimori, T.; Ohsumi, Y.; Tokuhisa, T.; Mizushima, N. The role of autophagy during the early neonatal starvation period. *Nature* **2004**, *432*, 1032–1036.